



Chemical Synthesis and X-ray Study of M-type Hexagonal Nano Ferrite Powders

Kersh R.M. and Al- Asbahi S.O.

Physics Department, Faculty of Science, Ibb University, Ibb, YEMEN

Available online at: www.isca.in

Received 5th March 2014, revised 1st April 2014, accepted 16th April 2014

Abstract

M-type hexagonal ferrites with composition $SrFe_{12-y}Mg_yO_{19-y/2}$ have been prepared by the co-precipitation method. The X-ray powder diffraction was employed to investigate their nanostructure constants. The X-ray data were analyzed using different softwares. The average values of lattice constants (a) and (c) are found in the range (5.867– 5.876) °Å and (22.918– 22.977) °Å respectively and the average crystallite size is found in the range 71 – 93 nm. $SrFe_{11.5}Mg_{0.5}O_{18.5}$ sample is the critical concentration where it has the minimum value of (a) lattice parameter, the minimum value of crystallite size and the maximum value of lattice strain.

Keywords: M- type hexagonal ferrites, nanostructure, lattice constants, crystallite size and lattice strain.

Introduction

Nanomaterials represent a novel class of materials in which a significant fraction of atoms is present on the surface that induces properties distinctly different from those of the normal polycrystalline materials^{1,2}. Nanoparticles due to their smaller size and large surface to volume ratio exhibit remarkable novel properties and methodical applications in the field of biotechnology, sensors, medical, catalysis, optical devices³. M-type strontium hexaferrite is considered a material with promising applications in the many fields such as: telecommunication, data recording, microwave devices and permanent magnets. This wide applications of SrM – type hexaferrites as a result of the following properties: relatively high values of magnetic anisotropy, electrical resistivity and Curie temperature in addition to possessing excellent chemical stability and corrosion resistivity^{4,5}. M-type hexa-ferrites belong to P63/mmc space group and crystallize in a hexagonal structure containing 64 ions per unit cell on 11 different symmetry sites. The 24 Fe atoms are distributed over five distinct sites: one tetrahedral site (4f1), three octahedral sites (12k, 2a, and 4f2) and one bipyramidal site (2b)^{6,7}. In order to improve the properties of $SrFe_{12}O_{19}$, some measures can be taken such as improving its microstructure, controlling its chemical composition, size and morphology^{8,9}. The chemical method provides better control on particle size distribution and chemical homogeneity^{10,11}. The co-precipitation method ensures proper distribution of various metal ions resulting into stoichiometric and smaller particles size product compared to some of the other chemical methods¹². The researchers have extensively studied the influence of partial Fe^{3+} substitution by Co^{2+} - Si^{4+} ¹³, Co^{2+} - Ti^{4+} ¹⁴, Mn^{2+} - Co^{2+} - Zr^{4+} ¹⁵, Co^{2+} - Ru^{4+} ¹⁶, Al^{3+} ¹⁷, Cr^{3+} ¹⁸, Ga^{3+} ¹⁹ and In^{3+} ²⁰ on the properties of M-type hexagonal ferrites. This work is an attempt to describe the fine

structure of nanocrystalline SrM – type hexagonal ferrites with composition $SrFe_{12-y}Mg_yO_{19-y/2}$ where, $y = 0, 0.25, 0.5, 0.57$ and 1 to elucidate the effect of magnesium ions on the lattice constants, the crystallite size and the lattice strain of the investigated samples.

Material and Methods

Nanocrystalline M-type series with composition $SrFe_{12-y}Mg_yO_{19-y/2}$ where, $y = 0, 0.25, 0.5, 0.75$ and 1, have been prepared by the co-precipitation method. The chemicals used for the synthesis of the investigated samples were $SrCl_2 \cdot 6H_2O$, $FeCl_3$ and $MgCl_2 \cdot 6H_2O$. The appropriate amounts of the salts were dissolved in de-ionized water. The solution of these precursors with molar ratio [(Fe + Mg)/Sr = 11] was prepared at room temperature. This solution was heated along with continuous stirring on hot plate. When temperature of solution was reached to 70°C, solution of NaOH was added until pH equal to 10.5 was achieved. The precipitate obtained was filtrated and washed for many times with de-ionized water and then dried in air at room temperature for one week. The dry precursors were ground well and then were sintered in an electrical furnace for 2 h at 1000°C by heat rate 4°C/min and were cooled to room temperature by the same rate. The X-ray powder diffraction patterns were carried out by using Scintag X-ray diffractometer ($k = 1.5418$ °Å). The recorded data of X-ray diffraction lines were performed at room temperature by step scanning method in 2h in the range 20.08° – 79.92°. The phases, the lattice constants and the physical structures of the hexagonal ferrite powders were calculated from X-ray diffractograms. CHEKCELL program and PEAKFIT software were used to refine the unit cell constants, and to identify and refine the peaks positions respectively. Williamson–Hall

method was used to determine the crystallite size and lattice strain.

Results and Discussion

Figure-1 shows the X-ray diffraction patterns of $\text{SrFe}_{12-y}\text{Mg}_y\text{O}_{19-y/2}$ that obtained at different substituted amounts of magnesium ions. From this figure we can notice that when Mg ions is equal to 0, 0.25 or 0.5, the samples has the single M-type hexagonal ferrites, whereas, when Mg ions is equal to 0.75 and 1, some of $\alpha\text{-Fe}_2\text{O}_3$ founded as an intermediate phase in the investigated samples. The relative intensities of the secondary phase increase beside phase of SrM – type hexaferrite with increasing of y Mg ions. The presence of $\alpha\text{-Fe}_2\text{O}_3$ phase beside M – type hexagonal ferrites is also reported in the previous papers²¹.

As shown in figure-2; lattice constant (c) increases monotonically with increasing of Mg ions whereas, the lattice constant (a) firstly increases with Mg ions up to $y = 0.5$, then decreases slightly as shown in Figure-3. Increasing of the lattice constant (c) with Mg ions (y) is due to replacement of smaller ionic radius (0.64 \AA) of ferric ions by higher ionic radius (0.65 \AA) of magnesium ions. Magnesium ions have a statistical distribution over tetrahedral and octahedral sites, but mainly prefer to occupy octahedral sites²². This means firstly, the magnesium ions go to the both octahedral and tetrahedral sites in the places of the ferric ions. This leads to increasing in (a) and (c) lattice constants with increasing of Mg ions (y). After that, when Mg ions (y) became higher than certain value $y = 0.5$, tetrahedral sites forbidden the addition magnesium ions, so it will be go to octahedral sites, this leads to continuously increasing of the lattice constant (c) with increasing of Mg ions (y). In this time, same number of ferric ions go to tetrahedral sites; some of these ions inter (with small radius than that of magnesium ions) to the grains of M – type phase and the residual collect at the grain boundaries and forming the secondary phase as shown in Figure-1 (the secondary phase presses on the tetrahedral sites in S block). This means decreasing of the lattice constant (a) with increasing of Mg ions (y). The values of the lattice constants a and c are in the range ($5.867 - 5.876 \text{ \AA}$) and ($22.918 - 22.977 \text{ \AA}$) respectively, which agree well with the reported values²³ for Sr-M-type.

Williamson–Hall method was used to determine the crystallite size and lattice strain. X-Ray Line Profile It is well known that if the sample is perfect and a perfect diffractometer has been used the diffraction peaks would be extremely sharp. Therefore, the broadening arises from two sources: instrumental contributions and sample contributions. It recognizes two main types of sample contribution broadening the size and strain components. Because of the nanocrystalline state of the studied samples, the sample contribution

broadening of the profiles was much higher than the instrumental broadening; therefore, instrumental correction was not applied in the evaluation²⁴. The size depends on the size of coherent domains and the second factor is caused by any lattice imperfection. We have used the residual peak fitting software, there are three AutoFit Peaks options offered by PeakFit. We have selected one of these options. In this option, the hidden peaks are detected by the “sharpening” achieved by deconvolving a Gaussian instrument response with the raw data. Baseline is also fitted with a Gaussian deconvolution procedure. We have used the standard cell constants for HBF as starting values for “CHEKCELL” program to identify the Bragg reflection. The average particle size for all investigated samples is given in Figure-4 as a function of y Mg ions. The data reveal that the crystallite size decreases with increasing of Mg ions (y) in the range 0 - 0.5. After that, the increasing trend of the crystallite size is achieved at Mg ions (y) becomes above 0.5. Decreasing of crystallite size with increasing of Mg ions (y) can be explained on the basis that; replacement of positive triple iron ions by positive divalent magnesium ions will be form new bonds between magnesium ions and oxygen ions and this will be reduce the number of negative oxygen ions (large size) and with a result decreasing of crystallite size. Increasing of crystallite size with increasing of magnesium ions for $y > 0.5$ may be under the secondary phase, which emergences with Mg ions (y) above 0.5 and presses on S blocks in X-Y plane but extended R block in the direction of Z-axis (easy direction of unit cell), as we have seen in the figure-2 and figure-3 of (a) and (c) lattice constants respectively. our investigated samples are much smaller in size (71 – 93) nm as compared to those prepared by glass crystallization method ($50\text{--}330 \text{ nm}$)²⁵ and by sol-gel method ($90\text{--}110 \text{ nm}$)²⁶ and $\text{SrFe}_{11.5}\text{Mg}_{0.5}\text{O}_{18.75}$ is the critical concentration where, it has the minimum value of crystallite size.

Figure-5 shows the lattice strain in the investigated samples as a function of Mg ions (y). From this figure can be seen that increasing of lattice strain with increasing of Mg ions (y) in the range 0 – 0.5. After that, the lattice strain decreases with increases of Mg ions (y). The minimum value of the lattice strain is found for undoped sample ($y = 0$) where, this sample has the natural arrangement of atoms in the unit cell. Increasing of Mg ions (y) leads to re-arrangement of the atoms and configure the appropriate bonds in the unit cell to ensure a balance of electrical charges. Hence, this mechanism leads to increasing of the lattice strain of the samples. When value of Mg ions (y) becomes greater than 0.5, the small quantities of the secondary phase appears between the nanocrystals and this character may be the reason of the decreasing of lattice strain with increasing of Mg ions (y) in the investigated samples.

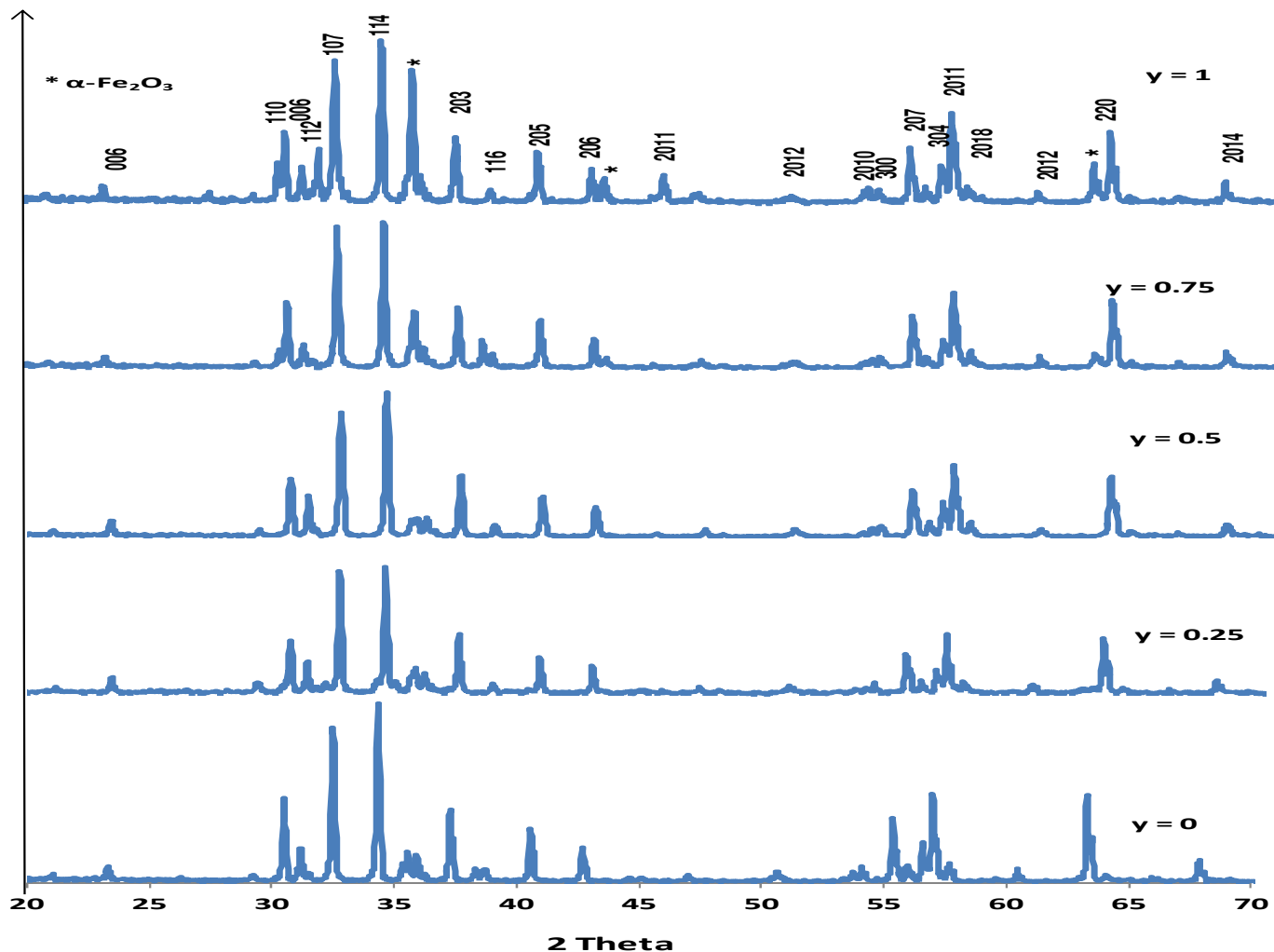


Figure-1
 X- ray diffraction pattern of $\text{SrFe}_{12-y}\text{Mg}_y\text{O}_{19-y/2}$ samples

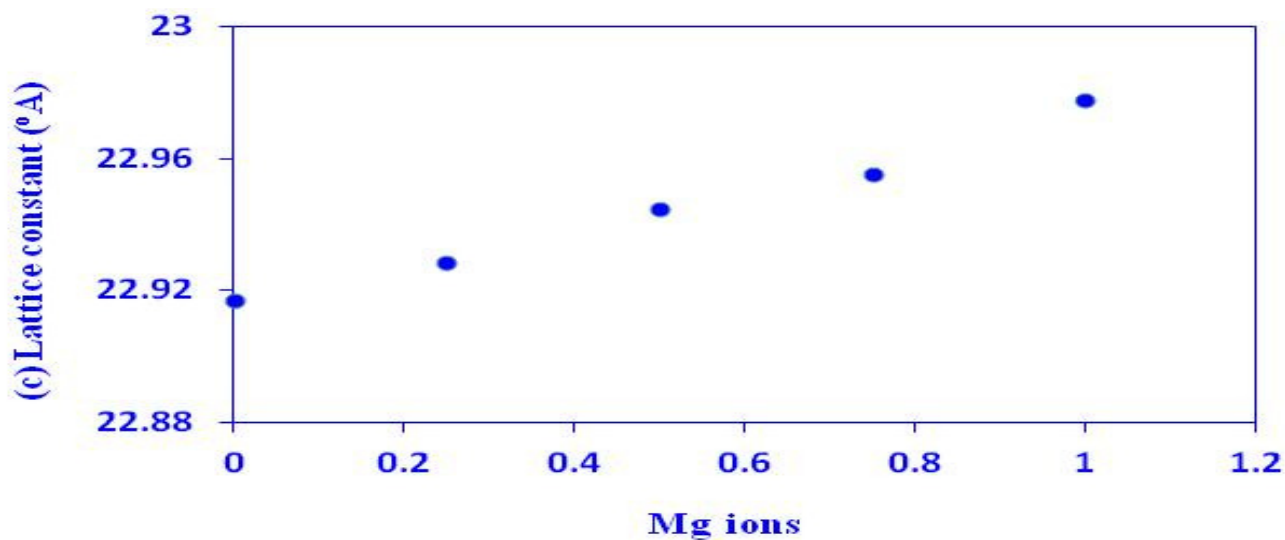


Figure-2
 The average value of lattice constant (c) of $\text{SrFe}_{12-y}\text{Mg}_y\text{O}_{19-y/2}$ as a function of Mg ions

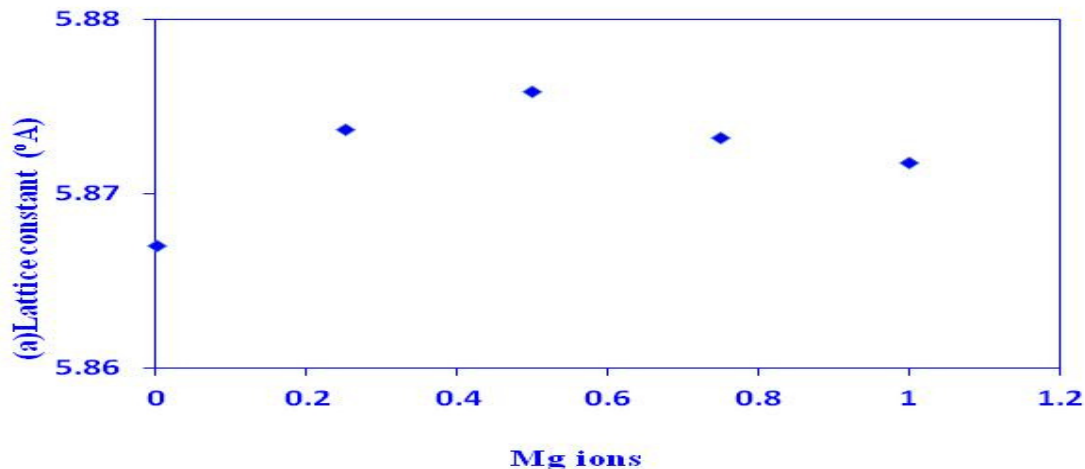


Figure-3
The average value of lattice constant (a) of $\text{SrFe}_{12-y}\text{Mg}_y\text{O}_{19-y/2}$ as a function of Mg ions

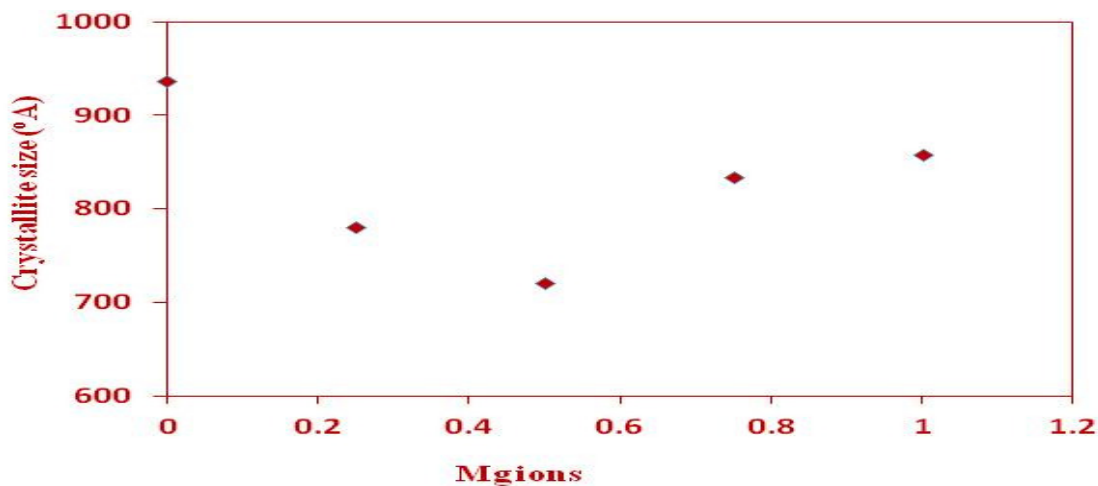


Figure-4
The average value of crystallite size of $\text{SrFe}_{12-y}\text{Mg}_y\text{O}_{19-y/2}$ as a function of Mg ions

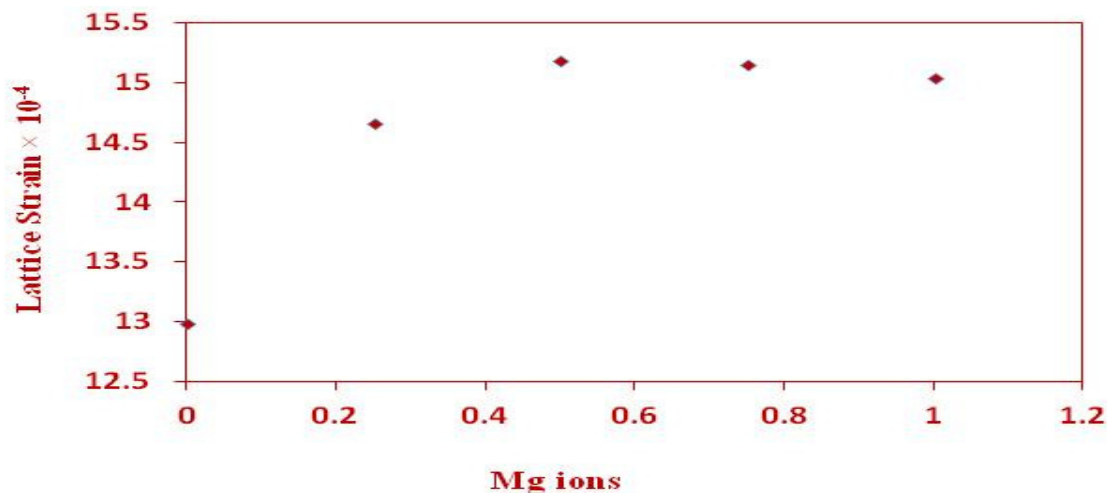


Figure-5
The average value of lattice strain of $\text{SrFe}_{12-y}\text{Mg}_y\text{O}_{19-y/2}$ as a function of Mg ions

Conclusion

Nanocrystalline M-type series with composition $\text{SrFe}_{12-y}\text{Mg}_y\text{O}_{19-y/2}$ where, $y = 0, 0.25, 0.5, 0.75$ and 1 , have been prepared by the co-precipitation method. X-ray diffraction pattern show that when the substituted amount y is equal to $0, 0.25$ or 0.5 , the samples are the single M-type hexagonal ferrites, whereas, when the substituted amount y is equal to 0.75 and 1 , some of $\alpha\text{-Fe}_2\text{O}_3$ founded as an intermediate phase in the investigated samples. Lattice constant (c) increases monotonically with increasing y Mg ions whereas, the lattice constant (a) at first increases with the substituted amount y , then decreases slightly. The crystallite size was in the range $71 - 93$ nm. $\text{SrFe}_{11.5}\text{Mg}_{0.5}\text{O}_{18.5}$ sample is the critical concentration where it has the minimum value of (a) lattice constant, the minimum value of crystallite size and the maximum value of lattice strain.

References

1. Singhal S., Garg A.N. and Chandra K., *J. Magn. Magn. Mater.*, **285**, 193–198 (2005)
2. Stefanescu M., Caizer C., Stoia M. and Stefanescu O., *Acta Mater*, **54**, 1249–1256 (2006)
3. Gnanasangeetha D. and Sarala Thambavani D., *Research Journal of Material Sciences*, **1(7)**, 1-8 (2013)
4. Dishovske N., Petkov A., Nedkov I. and Razkazov I., *IEEE Trans. Magn.*, **30**, 969–971 (1994)
5. Shrik B.T. and Buessem W.R., *J. Appl. Phys.*, **40**, 1294–1296 (1969)
6. Smit J., Wijn H.P.J., Ferrites, Philip's Tech. Library, New York, (1959)
7. Tang X., Yang Y. and Hu K., *J. Alloys Compd.*, **477**, 488–492 (2009)
8. Duan H.Z. and Li Q.L., *J. Mater. Sci. Eng.*, **25**, 179–183 (2007)
9. Du Y.W., Ferrite, Jiangsu Science and Technology Press, Nanjing (1995)
10. Rodriguez J.A. and Fernandez M., Garcia, John Wiley and Sons Inc, New York (2007)
11. Goldman A., Modern Ferrite Technology, second edition, Springer Science Business Media Inc. (2006)
12. Surrig C., Hempel K.A. and Bonnenberg D., *Appl. Phys. Lett.*, **74**, 2513 (1999)
13. Abbas S.M., Chatterjee R., Dixit A.K., Kumar A.V.R. and Goel T.C., *J. Appl. Phys.*, **101** (2007)
14. Tabatabaie F., Fathia M.H., Saatchia A. and Ghasemi A., *J. Alloys Compd.*, **474**, 206–209 (2009)
15. Ghasemi A. and Morisako A., *J. Alloys Compd.*, **456**, 485–491 (2008)
16. Pignard S., Vincent H., Flavin E. and Boust F., *J. Magn. Magn. Mater.*, **260**, 437–446 (2003)
17. Qiu J., Zhang Q. and Gu M., *J. Appl. Phys.*, **98**, 103905 (2005)
18. Ounnunkad S. and Winotai P., *J. Magn. Magn. Mater.*, **301**, 292–300 (2006)
19. Varadinov R., Nikolov V. and Peshev P., *J. Cryst. Growth*, **131**, 97–104 (1993)
20. Albanese G., Deriu A., Lucchini E. and Slokar G., *Appl. Phys. A Solids Surf.*, **26**, 45–50 (1981)
21. Xiansong Liu, Wei Zhong, Sen Yang, Zhi Yu, Benxi Gu and Youwei Du, *J. Magn. Magn. Mater.*, **238**, 207–214 (2002)
22. Ahmed M.A., Okasha N., Oaf M. and Kershi R.M., *J. Magn. Magn. Mater.*, **314**, 128–134 (2007)
23. Asghar G. and Rehman M. Anis-ur-, *J. Alloys Compd.*, **526**, 85–90 (2012)
24. Gubicza J., Nauyoks S., Balogh L., Zerda T.W. and Ungár T., *J. Materials Research*, **221**, 314 (2007)
25. Zhong W., Ding W., Zhang N., Hong J., Yan Q. and Du Y., *J. Magn. Magn. Mater.*, **168**, 196–202 (1997)
26. Rezlescu L., Rezlescu E., Popa P.D. and Rezlescu N., *J. Magn. Magn. Mater.*, **193**, 288–290 (1999)